


Energy conversion theorems for some linear steady states

L. A. Arias-Hernandez ^{1,*}, G. Valencia-Ortega ^{2,†}, C. R. Martinez-Garcia ^{3,‡} and F. Angulo-Brown ^{1,§}

¹*Departamento de Física, Escuela Superior de Física y Matemáticas, Instituto Politécnico Nacional, Ciudad de México 07738, México*

²*División de Matemáticas e Ingeniería, Facultad de Estudios Superiores Acatlán, Universidad Nacional Autónoma de México, Santa Cruz Acatlán, Naucalpan de Juárez 53150, México*

³*Departamento de Ciencias Básicas, Escuela Superior de Cómputo, Instituto Politécnico Nacional, Ciudad de México 07738, México*



(Received 7 July 2023; accepted 10 October 2023; published 5 January 2024)

One of the main issues that real energy converters present, when they produce effective work, is the inevitable entropy production. Within the context of nonequilibrium thermodynamics, entropy production tends to energetically degrade human-made or living systems. On the other hand, it is not useful to think about designing an energy converter that works in the so-called minimum entropy production regime since the effective power output and efficiency are zero. In this paper we establish some *energy conversion theorems* similar to Prigogine's theorem with constrained forces. The purpose of these theorems is to reveal trade-offs between design and the so-called operation modes for (2×2) -linear isothermal energy converters. The objective functions that give rise to those thermodynamic constraints show stability. A two-mesh electric circuit was built as an example to demonstrate the theorems' validity. Likewise, we reveal a type of energetic hierarchy for power output, efficiency, and dissipation function when the circuit is tuned to any of the operating regimes studied here. These are maximum power output (MPO), maximum efficient power (MP η), maximum omega function (M Ω), maximum ecological function (MEF), maximum efficiency (M η), and minimum dissipation function (mdf).

DOI: [10.1103/PhysRevE.109.014107](https://doi.org/10.1103/PhysRevE.109.014107)

I. INTRODUCTION

Since Prigogine formulated his principle of minimum entropy production in 1947 [1], also known as Prigogine's theorem, it has been subject to several controversies [2–7]. This theorem states that “in the linear regime, where the Onsager reciprocal relations are valid [8], all steady states in which unconstrained thermodynamic flows vanish are characterized by the following extremum principle: In the linear regime, the total entropy production in a system subject to flow of energy and matter, $d_i S/dt = \int \sigma dV$, reaches a minimum value at the non-equilibrium stationary state...” [9]. Despite the criticism received, Prigogine's theorem has prevailed mainly due to its experimental verification; for example, in the case of heat conduction in metallic rods [10,11], as well as computer simulations of the same system [12].

In their paper, to demonstrate the validity of Prigogine's theorem [12], Lurié and Wagensberg took as the only fixed force the temperature gradient $F_0 = T_h^{-1} - T_0^{-1}$, i.e., they considered extreme thermal reservoir temperatures of the rod. The rest of the $(n - 1)$ slices temperatures of their discrete model are used to construct the free forces F_j for $j = 1, 2, \dots, (n - 1)$. Under this assumption, they arrive to the minimum entropy production regime by following all the steps of the Prigogine procedure. It is important to note that

in Ref. [12], the so-called phenomenological coefficients L were used to represent the Fourier law in the one-dimensional form $J(x, t) = LX$, where $L = \kappa T^2$. That is, the thermal conductivity κ depends on T^{-2} , although, as was asserted by Jaynes [3], there is no known substance which obeys this relation. This obstacle was surmounted by Lurié and Wagensberg by considering that for small-enough temperature gradients the effects of taking $L = \kappa T^2$ are not important. This claim works reasonably. However, in Ref. [9], by means of the Euler-Lagrange formalism, the authors arrive at the function $T(x)$, which minimizes the entropy production and is linear with respect to x variable, by taking $L = \kappa T^2 \approx \kappa T_{av}^2$, where T_{av} is the average temperature of the rod. If the temperature gradient is small enough in the rod one will have that $T(x) = T_{av}[1 + \varepsilon(x)]$ with $|\varepsilon(x)| \ll 1$ [4]. For example, in Ref. [11] the corresponding experiment was performed for $\Delta T = 341.5 \text{ K} - 250 \text{ K} = 51.5 \text{ K}$ and for each case $|\varepsilon(x)| \sim 10^{-4}$ so that the above-mentioned approximation holds. More strong support of Prigogine's theorem was offered by Klein and Meijer, who proved it by using statistical mechanics methods [13]. They assumed a process consisting of mass and energy fluxes through a narrow tube that connects two containers of an ideal gas such as occurs when a gas is enclosed by rigid adiabatic walls, which at the same time is connected by means of a diathermic piston with a reservoir of both temperature and pressure. This type of systems reaches the final equilibrium state with their respective reservoirs without performing work. Something analogous happens in processes leading towards the steady state described in the previous heat conduction examples. In the case of the aforementioned gas interacting with the temperature and pressure reservoir, using the concept of thermodynamic availability and coupling

* Author to whom correspondence should be addressed: lar-ias@ipn.mx

† 903974@pcpuma.acatlan.unam.mx

‡ cmartinezga@ipn.mx

§ fangulob@ipn.mx

with a second system gives rise to the maximum useful work theorem [14,15]. Similarly, within the context of linear irreversible thermodynamics (LIT), a large number of steady states arise from the coupling of spontaneous processes and nonspontaneous ones. These couplings can exist in both living and human-made systems. Remarkably, this coupling concept can lead us to describe energy conversion processes in systems with constrained forces solely [16–18]. Caplan and Essig [17] developed a theory based on LIT for the study of linear biologic energy converters that work in steady states. These authors introduced concepts such as power output and efficiency to optimize the energy conversion process. Likewise, they took the usual notion of entropy production. Later, Stucki [16] used those ideas in the analysis of oxidative phosphorylation to establish other working regimes different than the minimum entropy production. In addition, Arias-Hernandez *et al.* [18] used concepts from finite-time thermodynamics to analyze the above-mentioned energy conversion process. It is clear that in heat conduction experiments subjected to small temperature gradients, the systems evolve towards a final steady state of minimal entropy production. Yet, as several authors have shown [16–20], in the case of two or more coupled processes, there are other steady states where certain quantities of interest to be optimized may come from natural or artificial needs.

The foregoing can translate into different proposals of trade-offs through characteristic functions, which are described in Sec. II of this article, i.e., thermodynamic mechanisms can be assumed whose goals are to maximize some energetic objective functions. Thus, at least five theorems similar to Prigogine’s can be stated (Sec. III) whose purpose is to show physical restrictions for (2×2) -linear isothermal energy converters to operate in some optimal and stable regimes. In Sec. IV, we design a two-mesh electrical circuit to exhibit nonzero energy conversion when the coupling of electrical currents meet the physical constraints imposed by these “energy conversion theorems” and experimental verification thereof is presented. Finally, our conclusions are exposed in Sec. V.

II. STEADY STATES WITHOUT MINIMUM ENTROPY PRODUCTION

Several phenomena in nature that are related to the transport of mass, charge, and energy have been described with a good approximation in the linear regime [8,21–23]. In general, the characteristic functions that have been defined to study nonequilibrium processes in a variety of human-made and living systems can be expressed in terms of sums of conjugate fluxes (J_i ’s) and forces (X_i ’s) [16–20,24,25]. The J_i ’s are the so-called thermodynamic fluxes, such as the strain rate, reaction speed, electrical current, rate of muscle contraction, etc. The X_i ’s are defined as the thermodynamic forces, such as the stress tensor, reaction affinities, electrochemical potential, muscle tension, etc.

Most of the previous simple linear relations are well known, for example, Ohm’s law for electrical current, Fick’s law for diffusion, the Fourier law for heat flow, etc. The main feature of these uncoupled processes promoted by unconstrained forces is their indisputable contribution to the

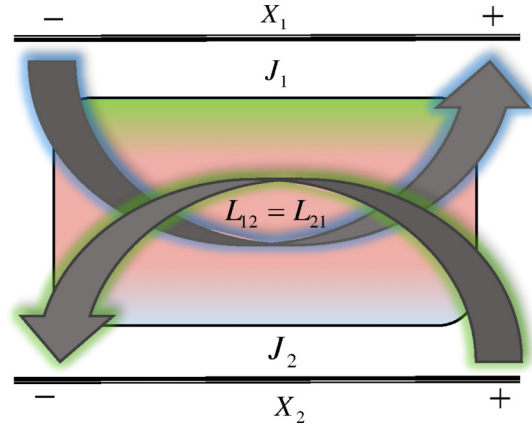


FIG. 1. Sketch of a simple isothermal energy converter (two coupled fluxes promoted by two conjugated forces), where $X_1 < 0$ is the force associated with the nonspontaneous flux, while $X_2 > 0$ is the other one related to the spontaneous flux.

increase of the system’s entropy and a decrease in its free energy, i.e., the unconstrained and spontaneous fluxes emulate simple diffusive and noninteracting processes [26,27]. However, there are other cases characterized by multiple interacting fluxes subjected to constrained forces. These types of phenomena involve energy conversion processes that can be classified into two sets of fluxes (see Fig. 1): the one associated with an entropy increase (spontaneous) and the one associated with a decrease of entropy (nonspontaneous) [18,28–30]. As an example to illustrate this, we can mention the transport of an ion across a cell membrane, which may be influenced not only by its electrochemical gradient but also by the influence of another gradient, such as an external pressure.

In general, to characterize the type of processes that occur in open thermodynamic systems one uses the so-called steady states. These steady states are typical of systems whose processes are kept constant on time, so the entropy created by the steady flow is more relevant than the entropy transferred to the surroundings [17,20,31,32],

$$\frac{dS_T}{dt} = \frac{dS_{\text{int}}}{dt} + \frac{dS_{\text{ext}}}{dt} > 0, \quad (1)$$

where $\dot{S}_{\text{int}} \equiv \sigma = \hat{J} : \hat{X}$ is usually called the entropy production while $\dot{S}_{\text{ext}} = 0$, since the entropy flux from the surroundings is equal to the entropy flux toward the system. That is, internal irreversibilities are responsible for the total entropy increments of the thermodynamic universe.

In the case of (2×2) -isothermal linear energy converter models, the entropy production is also a positive semidefinite quadratic form [8,9,17,18,20,21,28,33]:

$$\begin{aligned} \sigma &= J_1 X_1 + J_2 X_2 \\ &= (L_{11} X_1 + L_{12} X_2) X_1 + (L_{12} X_1 + L_{22} X_2) X_2 \\ &= [X_1, X_2] \begin{bmatrix} L_{11} & q\sqrt{L_{11}L_{22}} \\ q\sqrt{L_{11}L_{22}} & L_{22} \end{bmatrix} \begin{bmatrix} X_1 \\ X_2 \end{bmatrix} > 0, \quad (2) \end{aligned}$$

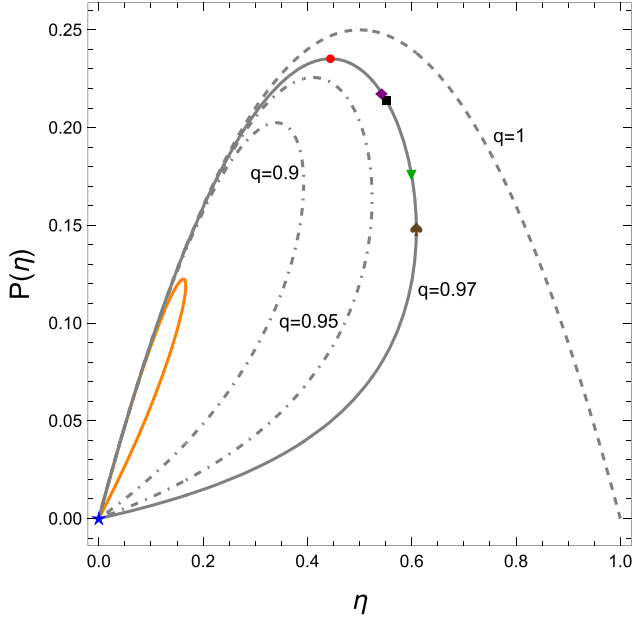


FIG. 2. Characteristic loops of power output versus efficiency of the (2×2) -energy converter for different values of the coupling coefficient q ; for the ideal case $q = 1$ a curve analogous to those of endoreversible thermodynamics (ET) is obtained (see Fig. 3 of Ref. [34]). Also, over the loop with $q = 0.97$ the points for the regimes maximum power output (MPO, red circle), maximum efficient power (MP_η , purple diamond), maximum omega function ($M\Omega$, black square), maximum ecological function (MEF, green inverted triangle), maximum efficiency ($M\eta$, brown spade), and minimum dissipation function (mdf, blue star) are marked from top to bottom along the loop. In addition, for the smallest loop (solid orange loop), with $q = 0.7$, it is observed that the model predicts an operating regime with almost no economic zone of interest; in the limit $q \rightarrow 0$ the EZI is null.

where the coefficient matrix \widehat{L} of this quadratic form is symmetric and q is given by

$$q = \frac{L_{12}}{\sqrt{L_{11}L_{22}}}, \quad (3)$$

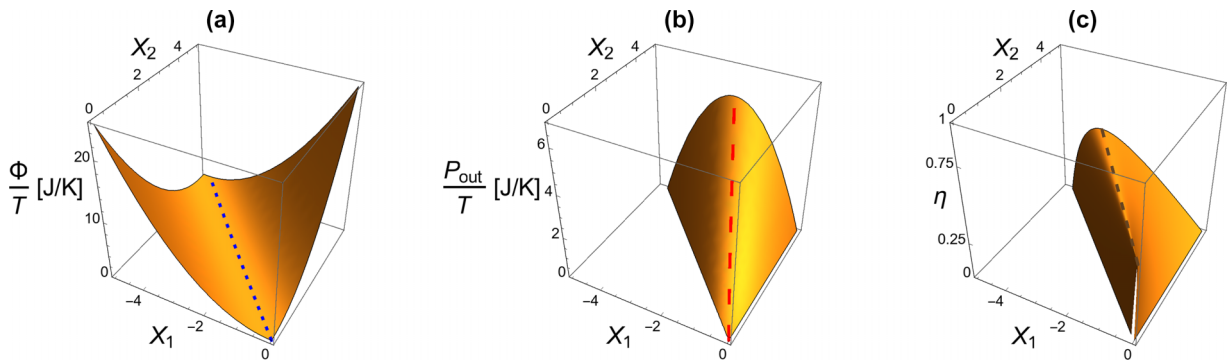


FIG. 3. Energetic functions versus X_1 (driven force) and X_2 (driver force) for an isothermal linear energy converter. (a) Normalized dissipation function, (b) normalized power output, and (c) efficiency, all of them plotted for a fixed value of $q = 0.97$. They reach their extreme values at $X_1^{\text{mdf}} = -\sqrt{L_{22}/L_{11}} X_2 q$ [dashed (small) blue line], $X_1^{\text{MPO}} = -\sqrt{L_{22}/L_{11}} X_2 q/2$ [dashed (large) red line], and $X_1^{\text{M}\eta} = -\sqrt{L_{22}/L_{11}} X_2 q/(1+\sqrt{1-q^2})$ [dashed (medium) brown line], respectively.

defined as the “degree of coupling” which fulfills $q^2 \in [0, 1]$, with $L_{11} > 0$ and $L_{22} > 0$. The practical interval of q is $[q_{\min}, 1]$ where q_{\min} guarantees the energy conversion and its quality [see the cross terms of Eq. (2) and Fig. 2] [16–18].

Since the purpose of those models is to describe energy conversion phenomena, three energetic functions (process variables) with extreme conditions can be defined: the dissipation function ($\Phi \equiv T\sigma$, with $T = \text{const}$ the absolute temperature of the converter), the power output ($P_O \equiv -TJ_1X_1$), and the efficiency ($\eta \equiv P_O/P_I = -TJ_1X_1/TJ_2X_2$) [16–18],

$$\Phi = (x^2 + 2qx + 1)TL_{22}X_2^2, \quad (4a)$$

$$P_O = -x(x + q)TL_{22}X_2^2, \quad (4b)$$

$$\eta = -\frac{(x + q)x}{qx + 1}. \quad (4c)$$

Here we have introduced a performance parameter,

$$x = \sqrt{\frac{L_{11}}{L_{22}}} \frac{X_1}{X_2}, \quad (5)$$

called the force ratio [35]. It measures the cross effect between the two potentials [17,18].

Under this linear energy converters scheme (see Fig. 1) [17,18,23], X_1 can be defined as the driven force while X_2 is the driver force, that is, $X_1 = X_1(q, X_2)$. Figure 3 shows the extremes in the three functions (Φ , P_O , and η) at different values of (X_1, X_2) , which are associated to three different operation modes: the minimum dissipation function (mdf), maximum power output (MPO), and maximum efficiency ($M\eta$). The optimal values adopted by x [Eq. (5)] for each of the process variables in Eq. (4) are

$$x^{\text{mdf}} = -q, \quad (6a)$$

$$x^{\text{MPO}} = -\frac{q}{2}, \quad (6b)$$

$$x^{\text{M}\eta} = -\frac{q}{1 + \sqrt{1 - q^2}}; \quad (6c)$$

consequently, other objective functions expressing different trade-offs between the energetic functions Φ , P_O , and η can be defined. They also have extreme values (see Fig. 4). The

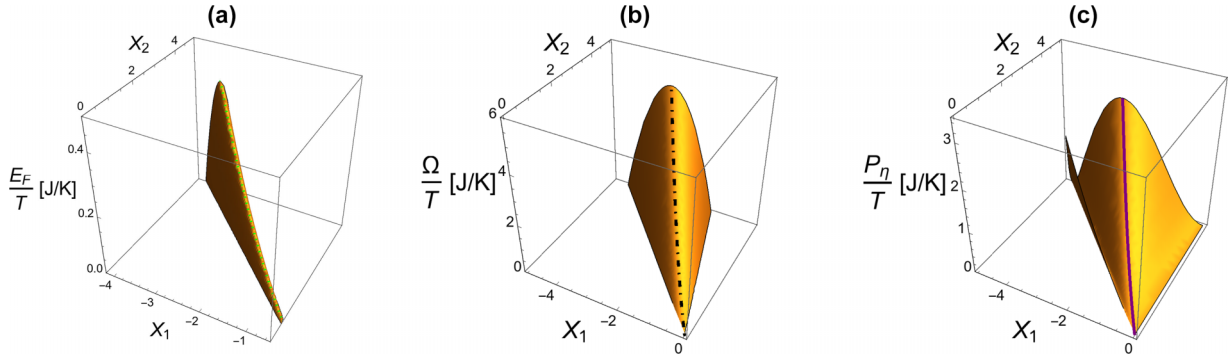


FIG. 4. Objective functions versus X_1 (driven force) and X_2 (driver force) for an isothermal linear energy converter. Normalized ecological function (a), normalized omega function (b), and normalized efficient power (c); all of them are plotted for a fixed value of $q = 0.97$. They reach their extreme values at X_1^{MEF} (dotted green line), $X_1^{\text{M}\Omega}$ (dot-dashed black line), and $X_1^{\text{MP}\eta}$ (solid purple line), respectively.

objective functions that we will study in order to characterize their optimal operation modes are [16,20,36]

$$E_F = -(2x^2 + 3xq + 1)TL_{22}X_2^2, \quad (7a)$$

$$\Omega = [\eta_M(qx + 1) - 2x(x + q)]TL_{22}X_2^2, \quad (7b)$$

$$P_\eta = \frac{[(x + q)x]^2}{qx + 1}TL_{22}X_2^2, \quad (7c)$$

where $E_F = P_O - \Phi$ is the ecological function [37]; $\Omega = (2 - \eta_M/\eta)P_O$ is the so-called omega function [36], with η_M the value of efficiency under the conditions that maximize it, i.e., Eq. (4c) evaluated at Eq. (6c); and $P_\eta = \eta P_O$ is the efficient power [16,38]. Each of the previous objective functions [Eqs. (4) and (7)] give us optimal performance modes, such as maximum ecological function (MEF), maximum Ω -function (M Ω), and maximum efficient power (MP η). For a linear energy converter their optima x values are

$$x^{\text{MEF}} = -\frac{3q}{4}, \quad (8a)$$

$$x^{\text{M}\Omega} = -\frac{q(4 - q^2 + 4\sqrt{1 - q^2})}{4(1 + \sqrt{1 - q^2})^2}, \quad (8b)$$

$$x^{\text{MP}\eta} = -\frac{4 + q^2 - \sqrt{16 - 16q^2 + q^4}}{6q}. \quad (8c)$$

The above-mentioned physically accessible characteristic points can be viewed in a P_O vs η plane (see marked regions over solid black loop for $q = 0.97$ in Fig. 2), similarly to the behavior of heat engines that operate in cycles between two thermal reservoirs [18,39].

A. Optimal performance modes within Φ vs η and P_O vs η spaces

In describing the performance of a linear energy converter, the process variables [Eqs. (4a)–(4c)] can define a configuration space to display all physically possible realizations. Then the parametric characteristic functions $\Phi = \Phi(\eta)$ and $P_O = P_O(\eta)$, for $q \in [q_{\min}, 1]$, allow us to note that the dissipation function has an inverse decreasing monotonous behavior, because when q decreases the limit value of Φ increases while η diminishes [18]. From the parametric graphs depicted in Refs. [18,30,40,41] and Fig. 2, we can observe that when the quality of the coupling between spontaneous and nonspontaneous fluxes is low, entropy production increases. In addition,

the well-known loop-shaped curves for heat engines [42] arise in LIT energy converters when $P_O = P_O(\eta, q)$. These loops intrinsically show the existence of extrathermodynamic conditions (see p. 126 of Ref. [43]) that dynamically constrain the processes of a linear energy converter. Each loop has two optimal points of interest [18,30], the one that corresponds to maximum- P_O point and the other one to maximum- η point, and between these two points the other performance regimes can be achieved [44]. This economic zone of interest (EZI) shows energy conversion with high power output, high efficiency, and low dissipated energy (see Fig. 2, solid black loop for $q = 0.97$).

When the operation modes associated with the three trade-off functions are evaluated in the so-called process variables (Φ, P_O, η) , the following hierarchies are established (see Appendix):

$$\Phi^{\text{mdf}} < \Phi^{\text{M}\eta} < \Phi^{\text{MEF}} < \Phi^{\text{M}\Omega} < \Phi^{\text{MP}\eta} < \Phi^{\text{MPO}}, \quad (9a)$$

$$P_O^{\text{mdf}} < P_O^{\text{M}\eta} < P_O^{\text{MEF}} < P_O^{\text{M}\Omega} < P_O^{\text{MP}\eta} < P_O^{\text{MPO}}, \quad (9b)$$

$$\eta^{\text{mdf}} < \eta^{\text{MPO}} < \eta^{\text{MP}\eta} < \eta^{\text{M}\Omega} < \eta^{\text{MEF}} < \eta^{\text{M}\eta}. \quad (9c)$$

The optimal performance regimes located between $[P_O^{\text{M}\eta}, P_O^{\text{MPO}}]$ can be reached when the force associated with the driven flux is tuned. This is achieved by means of the coupling coefficient and the force associated with the driver flux. That is, operation modes are linked with objective functions, which in principle can be built through the process variables.

III. ENERGY CONVERSION THEOREMS FOR SOME LINEAR STEADY STATES

In general, the validity limits for the hypotheses of LIT can be experimentally verified using several nonequilibrium systems characterized by continuous variables [9,11,45,46]. In particular, the Onsager relations have been shown to reflect the experimental results for small thermodynamic gradients, that is, the postulates of LIT are valid in situations close to some steady state [8,9,21,31,32].

In systems whose purely spontaneous processes are promoted by constrained thermodynamic forces, the entropy production will always adapt to a condition in which the characteristic steady state causes the same systems to dissipate the least energy possible to the surroundings (minimum entropy production's principle) [9,25,31,32]. On the other hand,

energy converters open up a range of physically accessible steady states that represent thermodynamic constraints under boundary conditions that correspond to optimal operating criteria [16,18–20,28,29]. These processes are characterized by a set of fixed forces ($X_i > 0$), associated with spontaneous fluxes, and another set of constrained forces ($X_j < 0$), subjected to an external condition and associated with non-spontaneous fluxes.

For the case of energy converters with two constrained forces and two coupled fluxes, a “constrained minimum entropy production theorem” can be claimed in terms of the dissipation function (Φ). This new proposal can be also stated as the “minimum dissipation function theorem” (mdf-THEOREM), as follows [33,41]:

mdf-THEOREM: When a nonequilibrium steady-state system is characterized by two generalized forces X_1 (associated with driven processes) and X_2 (associated with driver processes), it reaches and remains in a steady-state if the force X_2 is fixed. Then, under the condition of minimum dissipation function (mdf-regime), the driven flux J_1 vanishes.

Proof. Let us take the mathematical expression for dissipation function [Eq. (4a)]. By calculating the derivative of Φ with respect to X_1 assuming X_2 fixed, we obtain

$$\left(\frac{\partial\Phi}{\partial X_1}\right)_{X_2} = T[J_1 + L_{11}X_1 + q(\sqrt{L_{11}L_{22}})X_2] = 2TJ_1. \quad (10)$$

By hypothesis $(\frac{\partial\Phi}{\partial X_1})_{X_2} = 0$ and using the definition of J_1 [Eq. (2)], we get

$$J_1 = 0. \quad (11)$$

In order to establish a trade-off between the design and the operation mode of a linear energy converter, we will set out the following corollary that results from canceling the driven process.

mdf-COROLLARY: If the degree of coupling between the processes of a nonequilibrium steady-state system is $q = \frac{L_{12}}{\sqrt{L_{11}L_{22}}}$ and it is operating under the mdf-regime, then the cross effect between both generalized forces, given by the performance parameter $x = \sqrt{\frac{L_{11}}{L_{22}} \frac{X_1}{X_2}}$, is $x^{\text{mdf}} = -q$.

Proof. From the mdf-THEOREM, the constraint $J_1 = 0$ leads us to write the force X_1 as

$$X_1 = -q \left(\sqrt{\frac{L_{22}}{L_{11}}} X_2 \right). \quad (12)$$

By using the definition for the performance parameter x given by the Eq. (5) of Sec. II, we obtain

$$x^{\text{mdf}} = -q. \quad (13)$$

The steady states that can be identified within a linear energy converter correspond to the coupling of two observable processes, the so-called spontaneous and other nonspontaneous ones. This distinction was not fully addressed by Prigogine, since in the statement of his minimum entropy production principle, he made no distinction about the nature of

thermodynamic forces in energy transfer or energy conversion processes. In this work, we propose, by means of a simple step, the minimum dissipation function theorem for linear energy converters in steady state, i.e., the energetic version of the “constrained minimum entropy production theorem.” In fact, each of the optimization criteria presented in Sec. II satisfies a variational principle and can be represented by specific flux-force relations [27,47]. Thus, energy conversion processes can be associated with different stationary solutions. When the operation modes coincide, their steady states are adjusted to the same initial condition (the same degree of coupling q).

A. Similar theorems to the “constrained minimum entropy production theorem” for (2×2) -energy converters

As we have evidenced in Sec. II, in a large number of nonequilibrium steady-state processes that are carried out in both living and human-made systems, appropriate constraints (boundary conditions) can be found so that the energy conversion takes place in particular operation modes. If the purpose of the operation of an (2×2) -isothermal linear energy converter is to operate in optimal steady regimes with power output greater than zero, then these steady states can be established that lead the converter to the modes of operation described in Sec. I (MPO, $M\eta$, MEF, $M\Omega$, and $MP\eta$) [16,20,23,36,48] by choosing appropriate constrained forces. Such steady states (which are not of minimum entropy production) are identified by means of energy conversion theorems, as well as their corresponding corollaries, similarly to that of Prigogine’s minimum entropy production. The optimal regimes here analyzed were taken from the field of finite time thermodynamics (FTT) [18,49].

MPO-THEOREM: When a nonequilibrium steady-state system is characterized by two generalized forces X_1 (associated with driven processes) and X_2 (associated with driver processes), it reaches and remains in a steady state if the force X_2 is fixed. Then, under the condition of the maximum power output (MPO-regime), the driven flux J_1 is equal to $-L_{11}X_1$.

Proof. Let us consider the mathematical expression for power output [Eq. (4b)]. The partial derivative of P_{out} with respect to X_1 assuming X_2 fixed, is as follows:

$$\left(\frac{\partial P_{\text{O}}}{\partial X_1}\right)_{X_2} = -T(J_1 + L_{11}X_1). \quad (14)$$

By hypothesis $(\frac{\partial P_{\text{O}}}{\partial X_1})_{X_2} = 0$ at maximum power output, then we get

$$J_1 = -L_{11}X_1. \quad (15)$$

MPO-COROLLARY: If the degree of coupling between the processes of a nonequilibrium steady-state system is $q = \frac{L_{12}}{\sqrt{L_{11}L_{22}}}$ and it is operating under the MPO-regime, then the cross effect between both generalized forces, given by the performance parameter $x = \sqrt{\frac{L_{11}}{L_{22}} \frac{X_1}{X_2}}$, is $x^{\text{MPO}} = -\frac{q}{2}$.

Proof. From the MPO-THEOREM, we can substitute the constraint $J_1 = -L_{11}X_1$ into Eq. (2) and write the force X_1 as

$$X_1 = -\frac{q}{2} \left(\sqrt{\frac{L_{22}}{L_{11}}} X_2 \right). \quad (16)$$

By using the definition for the performance parameter x [Eq. (5) of Sec. II], we have

$$x^{\text{MPO}} = -\frac{q}{2}. \quad (17)$$

M η -THEOREM: When a nonequilibrium steady-state system is characterized by two generalized forces X_1 (associated with driven processes) and X_2 (associated with driver processes), it reaches and remains in a steady state if the force X_2 is fixed. Then, under the condition of the maximum efficiency (***M η -regime***), the driven flux J_1 is equal to $-(\frac{1-\eta}{1+\eta})L_{11}X_1$.

Proof. Let us take the mathematical expression for efficiency [Eq. (4c)]. By calculating the partial derivative with respect to X_1 assuming X_2 fixed, we obtain

$$\left(\frac{\partial \eta}{\partial X_1} \right)_{X_2} = -\frac{P_O}{P_I^2} \left(\frac{\partial P_I}{\partial X_1} \right) + \frac{1}{P_I} \left(\frac{\partial P_O}{\partial X_1} \right), \quad (18)$$

where P_I is the rate of incoming energy per temperature unit, this amount of energy being associated with spontaneous flux. The derivative $(\frac{\partial P_O}{\partial X_1})$ is given in the MPO-THEOREM, while $(\frac{\partial P_I}{\partial X_1})$ is

$$\left(\frac{\partial P_I}{\partial X_1} \right) = Tq\sqrt{L_{11}L_{22}}X_2. \quad (19)$$

Then, we can rewrite $(\frac{\partial \eta}{\partial X_1})_{X_2}$ as follows:

$$\left(\frac{\partial \eta}{\partial X_1} \right)_{X_2} = -\frac{T}{P_I} \left(\frac{P_O}{P_I} q\sqrt{L_{11}L_{22}}X_2 + J_1 + L_{11}X_1 \right). \quad (20)$$

By hypothesis $(\frac{\partial \eta}{\partial X_1})_{X_2} = 0$ and by using the definition of η [Eq. (4c)], we get

$$\eta(q\sqrt{L_{11}L_{22}}X_2 + L_{11}X_1 - L_{11}X_1) + J_1 + L_{11}X_1 = 0, \quad (21)$$

so that, finally,

$$J_1 = -\left(\frac{1-\eta}{1+\eta} \right) L_{11}X_1. \quad (22)$$

M η -COROLLARY: If the degree of coupling between the processes of a nonequilibrium steady-state system is $q = \frac{L_{12}}{\sqrt{L_{11}L_{22}}}$ and it is operating under the ***M η -regime***, then the cross effect between both generalized forces, given by the performance parameter $x = \sqrt{\frac{L_{11}}{L_{22}}} \frac{X_1}{X_2}$, is $x^{\text{M}\eta} = -\frac{q}{1+\sqrt{1-q^2}}$.

Proof. From the ***M η -THEOREM***, the constraint $J_1 = -(\frac{1-\eta}{1+\eta})L_{11}X_1$ leads us to write the force X_1 as

$$X_1 = -\frac{q(1+\eta)}{2} \left(\sqrt{\frac{L_{22}}{L_{11}}} X_2 \right). \quad (23)$$

By using the definition for x [Eq. (5)], as well as Eq. (4c), we have

$$x^{\text{M}\eta} = -\frac{q}{1+\sqrt{1-q^2}}. \quad (24)$$

1. Energy conversion theorems for trade-off functions

MEF-THEOREM: When a nonequilibrium steady-state system is characterized by two generalized forces X_1 (associated with driven processes) and X_2 (associated with driver processes), it reaches and remains in a steady state if the force X_2 is fixed. Then, under the condition of maximum ecological function (***MEF-regime***), the driven flux J_1 is equal to $-\frac{1}{3}L_{11}X_1$.

Proof. Let us consider the mathematical expression for the so-called ecological function [Eq. (7a)]. The partial derivative with respect to X_1 assuming X_2 fixed, is

$$\left(\frac{\partial E_F}{\partial X_1} \right)_{X_2} = -T(J_1 + L_{11}X_1 + 2J_1). \quad (25)$$

By hypothesis $(\frac{\partial E_F}{\partial X_1})_{X_2} = 0$, we get

$$J_1 = -\frac{1}{3}L_{11}X_1. \quad (26)$$

MEF-COROLLARY: If the degree of coupling between the processes of a nonequilibrium steady-state system is $q = \frac{L_{12}}{\sqrt{L_{11}L_{22}}}$ and it is operating under the ***MEF-regime***, then the cross effect between both generalized forces, given by the performance parameter $x = \sqrt{\frac{L_{11}}{L_{22}}} \frac{X_1}{X_2}$, is $x^{\text{MEF}} = -\frac{3q}{4}$.

Proof. From the ***MEF-THEOREM***, the constraint $J_1 = -\frac{1}{3}L_{11}X_1$ leads us to write the force X_1 as

$$X_1 = -\frac{3q}{4} \left(\frac{L_{22}}{L_{11}} X_2 \right). \quad (27)$$

By using the definition for x , we have

$$x^{\text{MEF}} = -\frac{3q}{4}. \quad (28)$$

M Ω -THEOREM: When a nonequilibrium steady-state system is characterized by two generalized forces X_1 (associated with driven processes) and X_2 (associated with driver processes), it reaches and remains in a steady state if the force X_2 is fixed. Then, under the condition of maximum omega function (***M Ω -regime***), the driven flux J_1 is equal to $-(\frac{2-\eta^{\text{M}\eta}}{2+\eta^{\text{M}\eta}})L_{11}X_1$.

Proof. Let us take the mathematical expression for the so-called omega function [Eq. (7b)]. By calculating the partial derivative of Ω with respect to X_1 and by assuming X_2 fixed,

$$\left(\frac{\partial \Omega}{\partial X_1} \right)_{X_2} = -T[(2 + \eta^{\text{M}\eta})J_1 + (2 - \eta^{\text{M}\eta})L_{11}X_1]. \quad (29)$$

By hypothesis $(\frac{\partial \Omega}{\partial X_1})_{X_2} = 0$. Then we obtain

$$J_1 = -\left(\frac{2 - \eta^{\text{M}\eta}}{2 + \eta^{\text{M}\eta}} \right) L_{11}X_1. \quad (30)$$

M Ω -COROLLARY: If the degree of coupling between the processes of a nonequilibrium steady-state system is $q =$

$\frac{L_{12}}{\sqrt{L_{11}L_{22}}}$ and it is operating under the $M\Omega$ -regime, then the cross effect between both generalized forces, given by the performance parameter $x = \sqrt{\frac{L_{11}}{L_{22}} \frac{X_1}{X_2}}$, is $x^{M\Omega} = -\frac{q(4-q^2+4\sqrt{1-q^2})}{4(1+\sqrt{1-q^2})^2}$.

Proof. From the $M\Omega$ -THEOREM, the constraint $J_1 = -\left(\frac{2-\eta^{M\eta}}{2+\eta^{M\eta}}\right)L_{11}X_1$ leads us to write the force X_1 as

$$X_1 = -\frac{q(2+\eta^{M\eta})}{4} \left(\sqrt{\frac{L_{22}}{L_{11}}} X_2 \right), \quad (31)$$

and by using the definition for x and $\eta^{M\eta} = \eta[x^{M\eta}(q), q]$, we obtain

$$x^{M\Omega} = -\frac{q(4-q^2+4\sqrt{1-q^2})}{4(1+\sqrt{1-q^2})^2}. \quad (32)$$

MP_η -THEOREM: When a nonequilibrium steady-state system is characterized by two generalized forces X_1 (associated with driven processes) and X_2 (associated with driver processes), it reaches and remains in a steady state if the force X_2 is fixed. Then, under the condition of maximum efficient power (MP_η -regime), the driven flux J_1 is equal to $-\left(\frac{2-\eta}{2+\eta}\right)L_{11}X_1$.

Proof. Let us consider the mathematical expression for the so-called efficient power [Eq. (7c)]. By calculating the partial derivative of P_η with respect to X_1 assuming X_2 fixed,

$$\left(\frac{\partial P_\eta}{\partial X_1} \right)_{X_2} = -\frac{TP_O}{P_I} \left[\frac{P_O}{P_I} L_{12} X_2 + 2(J_1 + L_{11} X_1) \right]. \quad (33)$$

By hypothesis $\left(\frac{\partial P_\eta}{\partial X_1} \right)_{X_2} = 0$ and by using the definition of η , we have

$$2J_1 + 2L_{11}X_1 + \eta(L_{12}X_2 + L_{11}X_1 - L_{11}X_1) = 0. \quad (34)$$

Finally,

$$J_1 = -\frac{2-\eta}{2+\eta} L_{11} X_1. \quad (35)$$

MP_η -COROLLARY: If the degree of coupling between the processes of a nonequilibrium steady-state system is $q = \frac{L_{12}}{\sqrt{L_{11}L_{22}}}$ and it is operating under the MP_η -regime, then the cross effect between both generalized forces, given by the performance parameter $x = \sqrt{\frac{L_{11}}{L_{22}} \frac{X_1}{X_2}}$, is $x^{MP_\eta} = \frac{4+q^2-\sqrt{q^4-16q^2+16}}{6q}$.

Proof. From the MP_η -THEOREM, the constraint $J_1 = -\frac{2-\eta}{2+\eta} L_{11} X_1$ leads us to write the force X_1 as

$$X_1 = -\frac{q(2+\eta)}{4} \left(\sqrt{\frac{L_{22}}{L_{11}}} X_2 \right). \quad (36)$$

By using the definitions for x and η , we get

$$x^{MP_\eta} = -\frac{4+q^2-\sqrt{q^4-16q^2+16}}{6q}. \quad (37)$$

TABLE I. Physical constraints on linear energy converters so that two or more steady states coincide with the minimum dissipation function condition.

Boundary Conditions	q
$\Phi_{\text{mdf}}(q) = \Phi_{\text{MPO}}(q)$	0
$\Phi_{\text{mdf}}(q) = \Phi_{\text{M}\eta}(q)$	0 and 1
$\Phi_{\text{mdf}}(q) = \Phi_{\text{MEF}}(q)$	0
$\Phi_{\text{mdf}}(q) = \Phi_{\text{M}\Omega}(q)$	0
$\Phi_{\text{mdf}}(q) = \Phi_{\text{MP}_\eta}(q)$	0

As has been pointed out in some works [50,51], a boundary condition that at the same time is linked to a particular dynamic performance mode has several stable steady solutions. The energetic optimization criteria presented in Sec. II can be equivalent when the degree of coupling between the flows adopt particular values. For instance, the steady state associated with the minimum dissipation function condition is identical to the other extreme criteria. In Table I these values of q are displayed. Other constraints can also be established using the previous corollaries and evaluating q in the characteristic functions presented in Sec. II.

All of the above energetic trade-offs fulfill the condition $\Phi > 0$, since the nonequilibrium steady states associated with them only appear when external thermodynamic forces are linked under an extreme condition. Thus, the operation modes involve the maintenance of steady states for coupled processes that waste free energy at different rates.

B. Temporal evolution of the characteristic functions and stability of their steady states

The analysis of external perturbations on different types of thermal cycle models has been topic of interest [52–55]. Since thermal engines operate with many cycles per unit time, the effect of noisy perturbations forces us to have a well-design systems guaranteeing stability in their operating regimes (steady-state regimes) [56–58]. In several analyses on LIT [9,31,59–61], it has been shown that spontaneous fluctuations on a particular steady state drive the system backs to its condition of *minimum entropy production*. In this subsection we show that the stability of linear steady states can be also attained for the constrained cases.

1. Temporal evolution of the dissipation function

For the case of (2×2) -isothermal energy converters, let us consider the dissipation function $\Phi = \Phi(X_i, J_i)$ in a arbitrary nonequilibrium steady state. As $\Phi = T \int_V (J_1 X_1 + J_2 X_2) dV$, the time variation of Φ can be written as

$$\begin{aligned} \frac{d\Phi}{dt} &= T \int_V \left(J_1 \frac{dX_1}{dt} + J_2 \frac{dX_2}{dt} \right) dV \\ &+ T \int_V \left(X_1 \frac{dJ_1}{dt} + X_2 \frac{dJ_2}{dt} \right) dV \\ &\equiv \frac{d_X \Phi}{dt} + \frac{d_J \Phi}{dt}, \end{aligned} \quad (38)$$

where $d_X \Phi/dt$ is the time variation of thermodynamic forces associated with spontaneous and nonspontaneous fluxes and $d_J \Phi/dt$ is the temporal change of these conjugated fluxes. In the linear regime, where the Onsager reciprocal relations ($L_{ij} =$

L_{ji}) are fulfilled, a general property has been stated [9,31,59]. Then from Eq. (38) can be write as

$$\begin{aligned} \frac{d_j \Phi}{dt} &= T \int_V \left[\sum_{k=1}^2 \left(X_1 L_{1k} \frac{dX_k}{dt} + X_2 L_{2k} \frac{dX_k}{dt} \right) \right] dV \\ &= T \int_V \left(J_1 \frac{dX_1}{dt} + J_2 \frac{dX_2}{dt} \right) dV = \frac{d_X \Phi}{dt} \\ &= \frac{1}{2} \frac{d\Phi}{dt}. \end{aligned} \quad (39)$$

If we assume hereinafter homogeneity and unitary volume, then the time derivative of each X_i can be written by considering that extent variables (a_k) of the thermodynamic system can evolve in time,

$$\frac{dX_i}{dt} = \sum_k \left(\frac{\partial X_i}{\partial a_k} \right) \frac{da_k}{dt}. \quad (40)$$

Thus, from Eqs. (38) and (39) several authors shown (see Refs. [9,31,32]), that

$$\frac{d\Phi}{dt} = 2T \left[J_1 \sum_{k=1}^2 \left(\frac{\partial X_1}{\partial a_k} \right) J_k + J_2 \sum_{k=1}^2 \left(\frac{\partial X_2}{\partial a_k} \right) J_k \right] < 0. \quad (41)$$

In this inequality we separately show the contributions to the temporal evolution of dissipation, the one associated with the managed flow and the one associated with the driving flow, considering the Onsager reciprocity relations and the definition of $da_k/dt \equiv J_k$. Since $J_2 > J_1 \geq 0$ and each J_k is in general a linear combination of these, the sign of the terms in Eq. (41) depends on the signs of the partial derivatives $\partial X_i / \partial a_k$. It can be ensured that $\partial X_2 / \partial a_k$ is negative, because the equilibrium state is an attractor and in its neighborhood the time evolution of the converter is in the direction of the decrease in force X_2 . On the other hand, since $P_O \geq 0$ then it is guaranteed that $|\partial X_1 / \partial a_k| \leq |\partial X_2 / \partial a_k|$ and inequality Eq. (41) is fulfilled. This means that in any operation regime the temporal evolution of the dissipation function is decreasing.

2. Temporal evolution of the power output

In the same way, given an arbitrary volume, let us now consider the power output for a (2×2) -isothermal energy converter $P_O = P_O(X_i, J_i)$. Then, the time variation of P_O is

$$\begin{aligned} \frac{dP_O}{dt} &= -T \left(\int_V J_1 \frac{dX_1}{dt} dV + \int_V X_1 \frac{dJ_1}{dt} dV \right) \\ &\equiv - \left(\frac{d_X P_O}{dt} + \frac{d_J P_O}{dt} \right) \end{aligned} \quad (42)$$

and under the same mathematical assumptions of Refs. [9,31,59], we can find that

$$\frac{d_J P_O}{dt} < \frac{d_X P_O}{dt}, \quad (43)$$

and by using the condition given by Eq. (40) in Eq. (42), we have

$$\frac{dP_O}{dt} = -\frac{d\Phi}{dt} + T \left(J_2 \frac{dX_2}{dt} + X_2 \frac{dJ_2}{dt} \right)$$

$$\begin{aligned} &= -T \left[(J_1 + L_{11}X_1) \sum_{k=1}^2 \left(\frac{\partial X_1}{\partial a_k} \right) J_k \right. \\ &\quad \left. + (J_2 - L_{22}X_2) \sum_{k=1}^2 \left(\frac{\partial X_2}{\partial a_k} \right) J_k \right]. \end{aligned} \quad (44)$$

Therefore, as $|L_{11}X_1| < |L_{22}X_2|$ then $(J_1 + L_{11}X_1) > (J_2 - L_{22}X_2)$. In the neighborhood of the equilibrium state, it is also fulfilled that

$$\frac{dP_O}{dt} < 0. \quad (45)$$

This new constraint guarantees the stability of a steady state linked to the power output regime.

3. Temporal evolution of the efficiency

For the case of the efficiency in this type of linear energy converters, $\eta = \eta(X_i, J_i)$. The temporal evolution of η can be written analogously to Φ and P_O as

$$\frac{d\eta}{dt} \equiv -\frac{1}{P_I^2} \left[P_I \frac{d\Phi}{dt} - \Phi \left(\frac{d_X P_I}{dt} + \frac{d_J P_I}{dt} \right) \right]; \quad (46)$$

since $P_O = -\Phi + P_I$. Now the following mathematical constraints give rise to:

$$|P_O| < |P_I|, \quad (47a)$$

$$\frac{d_X P_I}{dt} < \frac{d_J P_I}{dt}, \quad (47b)$$

and by considering Eq. (40),

$$\begin{aligned} \frac{d\eta}{dt} &= -\frac{1}{P_I^2} \left\{ P_I \left(\frac{d\Phi}{dt} \right) \right. \\ &\quad - \Phi \left[(J_1 - L_{11}X_1) \sum_{k=1}^2 \left(\frac{\partial X_1}{\partial a_k} \right) J_k \right. \\ &\quad \left. \left. + (J_2 + L_{22}X_2) \sum_{k=1}^2 \left(\frac{\partial X_2}{\partial a_k} \right) J_k \right] \right\}, \end{aligned} \quad (48)$$

since $L_{12}X_2 = J_1 - L_{11}X_1$, in the neighborhood of the equilibrium state:

$$\frac{d\eta}{dt} < 0, \quad (49)$$

because of $(J_1 - L_{11}X_1) < (J_2 + L_{22}X_2)$. Once again, this new constraint describes the stability of a steady state with respect to this energetic function.

4. Temporal evolution of the trade-off functions

Finally, let us take the mathematical expressions of the three objective functions ecological function, omega function, and efficient power in order to analyze the effect of the fluctuations around their respective stable state.

a. Temporal evolution of E_F . For the (2×2) -linear system, in the ecological regime $E_F = E_F(X_i, J_i)$, its temporal evolution when it is disturbed, can be studied from

$$\frac{dE_F}{dt} = -T \left[2 \left(\frac{d_X P_O}{dt} + \frac{d_J P_O}{dt} \right) + \frac{d_X P_I}{dt} + \frac{d_J P_I}{dt} \right]. \quad (50)$$

By Eqs. (39) and (43), we can state that

$$\frac{dJ E_F}{dt} < \frac{dX E_F}{dt}, \quad (51)$$

and by using the definition of Eq. (40) as well as Eqs. (41) and (44),

$$\begin{aligned} \frac{dE_F}{dt} = -T \left[(3J_1 + L_{11}X_1) \sum_{k=1}^2 \left(\frac{\partial X_1}{\partial a_k} \right) J_k \right. \\ \left. + (3J_2 - L_{22}X_2) \sum_{k=1}^2 \left(\frac{\partial X_2}{\partial a_k} \right) J_k \right]. \quad (52) \end{aligned}$$

Then, in the vicinity of the equilibrium state,

$$\frac{dE_F}{dt} < 0. \quad (53)$$

b. Temporal evolution of Ω . Now let us consider the omega function $\Omega = \Omega(X_i, J_i)$; its temporal variation is

$$\frac{d\Omega}{dt} = -T \left[2 \left(\frac{d_X P_O}{dt} + \frac{d_J P_O}{dt} \right) + \eta_M \left(\frac{d_X P_I}{dt} + \frac{d_J P_I}{dt} \right) \right]. \quad (54)$$

Equations (39) and (43) allow us to establish that

$$\frac{dJ \Omega}{dt} < \frac{dX \Omega}{dt}, \quad (55)$$

then, taking the expressions given by Eqs. (40) and (44),

$$\begin{aligned} \frac{d\Omega}{dt} = -T \left\{ [(2 + \eta_M)J_1 + (2 - \eta_M)L_{11}X_1] \sum_{k=1}^2 \left(\frac{\partial X_1}{\partial a_k} \right) J_k \right. \\ \left. + [(2 + \eta_M)J_2 - (2 - \eta_M)L_{22}X_2] \sum_{k=1}^2 \left(\frac{\partial X_2}{\partial a_k} \right) J_k \right\}. \quad (56) \end{aligned}$$

Once again, in the zone near the equilibrium state

$$\frac{d\Omega}{dt} < 0. \quad (57)$$

c. Temporal evolution of P_η . Finally, let us use the mathematical expression for the efficient power $P_\eta = P_\eta(X_i, J_i)$. The temporal evolution of this objective function is

$$\frac{dP_\eta}{dt} = \frac{TP_O}{P_I^2} \left[2P_I \left(\frac{d_X P_O}{dt} + \frac{d_J P_O}{dt} \right) - P_O \left(\frac{d_X P_I}{dt} + \frac{d_J P_I}{dt} \right) \right]. \quad (58)$$

Due to the validity of Eqs. (39) and (43), we can state that

$$\frac{dJ P_\eta}{dt} < \frac{dX P_\eta}{dt}, \quad (59)$$

by taking into account the constraints [Eqs. (44) and (47)], in the neighborhood of the equilibrium state:

$$\frac{dP_\eta}{dt} < 0. \quad (60)$$

Inequalities (52), (57), and (60) express new constraints that describe the stability of three steady states associated with three different objective functions.

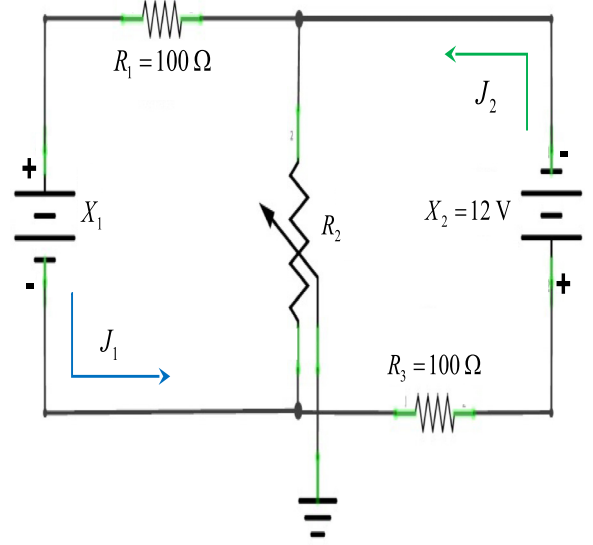


FIG. 5. Two-mesh resistive electric circuit, modeled as a (2×2) -simple isothermal energy converter. In this case, the voltage source X_1 is associated with the nonspontaneous flux J_1 (electric current), while the fixed voltage source X_2 is related to the spontaneous flux J_2 (electric current).

The above-mentioned conditions ensure the stability of isothermal energy converters, whose energetic processes occur in the linear regime when small perturbations are considered. As the so-called characteristic functions are positive and also their respective temporal variation are negative, they constitute the so-called Lyapunov conditions [60] and guarantee the stability of any dynamic state. Those states are considered simple attractors when the systems experience energetic fluctuations.

IV. AN APPLICATION OF ENERGY THEOREMS: ELECTRIC CIRCUIT WITH RESISTIVE ELEMENTS AND TWO COUPLED FLUXES

In this section, we apply the previous results, associated with steady states without minimum entropy production, to study the energetics for a (2×2) -isothermal linear energy converter consisting of an electric circuit of two meshes with passive elements (resistors) and powered by two dc voltage sources (see Fig. 5). Through Kirchhoff's equations that describe the energy conservation between the meshes, within the context of generalized flows and forces, we found the so-called cross effect ($L_{12} = L_{21}$) is fulfilled. Then, from the parameters related to its design (q) and its operation modes (x), we can characterize all the optimal operating criteria that correspond to particular stationary states.

A. Dynamic equations of the resistive circuit

Let us consider that the electric currents involved are time independent, with J_1 the driven flux that flows through the mesh 1 and J_2 the driver flux that flows through the mesh 2. In addition, X_1 and X_2 are the dc voltage sources that promote the fluxes. As the circuit phenomenological equations can be

associated with the Kirchhoff laws, then for the mesh 1 (left side in Fig. 5) we have

$$X_1 = (R_1 + R_2)J_1 - R_2J_2, \quad (61)$$

while for the mesh 2 (right side of Fig. 5)

$$X_2 = (R_2 + R_3)J_2 - R_2J_1. \quad (62)$$

In order to study the phenomenological equation of this system in the Onsager context, we must reverse Eqs. (61) and (62), i.e., writing (J_1, J_2) in terms of (X_1, X_2) . Hence,

$$\begin{pmatrix} J_1 \\ J_2 \end{pmatrix} = \begin{pmatrix} \frac{R_2+R_3}{\Delta} & \frac{R_2}{R_1+R_2} \\ \frac{R_2}{\Delta} & \frac{R_2}{\Delta} \end{pmatrix} \begin{pmatrix} X_1 \\ X_2 \end{pmatrix}, \quad (63)$$

where $\Delta = R_1(R_2 + R_3) + R_2R_3$ and $X'_{1,2} = X_{1,2}/T$. Note that the system of equations [Eq. (63)] represents the generalized Onsager equations whose equality in the crossed coefficients represents the contribution of each force X_i with the flux $J_{k \neq i}$. In this case, the parameter q is related to the intrinsic features of the circuit, and it can be rewritten in terms of the resistive elements nominal values as follows:

$$q = \frac{L_{12}}{\sqrt{L_{11}L_{22}}} = \frac{R_2}{\sqrt{\Delta + R_2^2}}. \quad (64)$$

The force ratio x which has all the extrathermodynamic information of the system takes the mathematical expression:

$$x = \sqrt{\frac{L_{11} X_1}{L_{22} X_2}} = \sqrt{\frac{R_2 + R_3}{R_1 + R_2} \frac{X_1}{X_2}}. \quad (65)$$

In the following, we will study every optimization criteria in terms of arbitrary values that the resistors can adopt, with the aim not only of characterizing the steady state related to an optimal coupling in the circuit's stable configuration but also of ensuring that the system adapts to the selected operating regime.

B. Steady state of minimum dissipation function (mdf)

From the mdf-THEOREM it follows that $x^{\text{mdf}} = -q$ can be rewritten by substituting Eq. (64) into Eq. (65) to get

$$x^{\text{mdf}} = -\frac{R_2}{\sqrt{\Delta + R_2^2}}. \quad (66)$$

Then, the force X_1 is rewritten in this regime as

$$X_1^{\text{mdf}} = -\frac{R_2}{R_2 + R_3} X_2. \quad (67)$$

Thus, the energetics under mdf operation regime is

$$\Phi^{\text{mdf}} = \frac{TX_2^2}{R_2 + R_3}, \quad (68a)$$

$$P^{\text{mdf}} = 0, \quad (68b)$$

$$\eta^{\text{mdf}} = 0. \quad (68c)$$

C. Steady state of maximum power output (MPO)

By applying the MPO-THEOREM to the circuit of Fig. 5, we find that $x^{\text{MPO}} = -\frac{q}{2}$ can be written as

$$x^{\text{MPO}} = -\frac{R_2}{2\sqrt{\Delta + R_2^2}}, \quad (69)$$

and thereby the force X_1 acquires the form

$$X_1^{\text{MPO}} = -\frac{R_2}{2(R_2 + R_3)} X_2. \quad (70)$$

The energetics beneath MPO operation regime is

$$\Phi^{\text{MPO}} = \left[\frac{4\Delta + R_2^2}{4(R_2 + R_3)\Delta} \right] TX_2^2, \quad (71a)$$

$$P^{\text{MPO}} = \left[\frac{R_2^2}{4(R_2 + R_3)\Delta} \right] TX_2^2, \quad (71b)$$

$$\eta^{\text{MPO}} = \frac{R_2^2}{4\Delta + 2R_2^2}. \quad (71c)$$

D. Steady state of maximum efficiency (M η)

By taking the M η -THEOREM, we have that $x^{\text{M}\eta}$ is given in terms of the resistors values as

$$x^{\text{M}\eta} = -\frac{R_2}{\sqrt{\Delta + R_2^2} + \sqrt{\Delta}}, \quad (72)$$

so that the force associated with the driven flux X_1 takes the form:

$$X_1^{\text{M}\eta} = -\frac{R_2}{(R_2 + R_3) + \sqrt{\frac{\Delta}{R_1 + R_2}}} X_2. \quad (73)$$

Therefore, the energetics that results in the M η -regime is

$$\Phi^{\text{M}\eta} = \frac{2TX_2^2}{(R_2 + R_3)(1 + \sqrt{\Gamma})}, \quad (74a)$$

$$P^{\text{M}\eta} = \frac{TX_2^2 R_2^2}{\sqrt{(R_2 + R_3)(\Delta + R_2^2)} \Delta (1 + \sqrt{\Gamma})^2}, \quad (74b)$$

$$\eta^{\text{M}\eta} = \frac{R_2^2 \sqrt{C}}{2(1 + \sqrt{\Gamma})(R_1 + R_3) + R_2^2 \sqrt{\Gamma}}, \quad (74c)$$

$$\text{with } \sqrt{\Gamma} = \sqrt{\frac{\Delta}{\Delta + R_2^2}}.$$

E. Steady state of maximum ecological function (MEF)

From the MEF-THEOREM, it can be shown that $x^{\text{MEF}} = -\frac{3}{4}q$ is given in terms of the circuit elements [Eq. (64)] as

$$x^{\text{MEF}} = -\frac{3R_2}{4\sqrt{\Delta + R_2^2}}, \quad (75)$$

and then the force X_1 associated with the nonspontaneous flux is

$$X_1^{\text{MEF}} = -\frac{3R_2}{4(R_2 + R_3)} X_2, \quad (76)$$

and the energetics corresponding to the MEF regime remains,

$$\Phi_{\text{MEF}} = \left[\frac{16\Delta + R_2^2}{16(R_2 + R_3)\Delta} \right] T X_2^2, \quad (77a)$$

$$P_{\text{MEF}} = \left[\frac{3R_2^2}{16(R_2 + R_3)\Delta} \right] T X_2^2, \quad (77b)$$

$$\eta_{\text{MEF}} = \frac{3R_2^2}{4\Delta + R_2^2}. \quad (77c)$$

F. Steady state of maximum omega function (M Ω)

By using the M Ω -THEOREM, it is derived that $x^{\text{M}\Omega} = -\frac{q(4-q^2+4\sqrt{1-q^2})}{4(1+\sqrt{1-q^2})}$ [Eq. (32)] can also be written as

$$x^{\text{M}\Omega} = -\frac{R_2(3 + \Gamma + 4\sqrt{\Gamma})}{4\sqrt{\Delta + R_2^2}(1 + \sqrt{\Gamma})^2}, \quad (78)$$

in order to characterize the force X_1 ,

$$X_1^{\text{M}\Omega} = -\frac{R_2(3 + \Gamma + 4\sqrt{\Gamma})}{4(R_2 + R_3)(1 + \sqrt{\Gamma})^2} X_2. \quad (79)$$

Thus, the energetics is evaluated in the M Ω regime as

$$\Phi^{\text{M}\Omega} = \frac{(R_1 + R_2)T X_2^2}{\Delta} \times \left\{ \sqrt{\Gamma} + (1 - \Gamma) \left[\frac{(3 + \Gamma + 4\sqrt{\Gamma})^2}{16(1 + \sqrt{\Gamma})^4} - \frac{1}{2} \right] \right\}, \quad (80a)$$

$$P^{\text{M}\Omega} = \frac{T X_2^2 R_2^2 (3 + \Gamma + 4\sqrt{\Gamma})(1 + 3\Gamma + 4\sqrt{\Gamma})}{16(R_2 + R_3)\Delta(1 + \sqrt{\Gamma})^4}, \quad (80b)$$

$$\eta^{\text{M}\Omega} = \frac{R_2^2(3 + \Gamma + 4\sqrt{\Gamma})(1 + 3\Gamma + 4\sqrt{\Gamma})}{8(\Delta + R_2^2)(1 + \sqrt{\Gamma})^4(1 + \Gamma - \sqrt{\Gamma})}. \quad (80c)$$

G. Steady state of maximum efficient power (MP $_{\eta}$)

Finally, by means of the MP $_{\eta}$ -THEOREM, the forces ratio $x^{\text{MP}_{\eta}} = -\frac{4+q^2-\sqrt{q^4-16q^2+16}}{6q}$ can be rewritten by using Eq. (64) as

$$x^{\text{MP}_{\eta}} = -\frac{5 - \Gamma - \sqrt{16\Gamma + (1 - \Gamma)^2}}{6q}, \quad (81)$$

from which X_1 is given by

$$X_1^{\text{MP}_{\eta}} = -\frac{(R_1 + R_2)[5 - \Gamma - \sqrt{16\Gamma + (1 - \Gamma)^2}]}{6R_2} X_2. \quad (82)$$

Accordingly, the energetics of the system in the MP $_{\eta}$ regime is

$$\Phi^{\text{MP}_{\eta}} = \frac{(R_1 + R_2)T X_2^2}{\Delta} \left\{ 1 + \frac{(\Delta + R_2^2)[5 - \Gamma - \sqrt{16\Gamma + (1 - \Gamma)^2}]^2}{36R_2^2} - \frac{[5 - \Gamma - \sqrt{16\Gamma + (1 - \Gamma)^2}]}{3} \right\}, \quad (83a)$$

$$P^{\text{MP}_{\eta}} = \frac{T X_2^2 (R_1 + R_2)[5 - \Gamma - \sqrt{16\Gamma + (1 - \Gamma)^2}][6R_2^2 + \Delta(\sqrt{16\Gamma + (1 - \Gamma)^2}) - 4]}{36R_2^2 \Delta}, \quad (83b)$$

$$\eta^{\text{MP}_{\eta}} = \frac{[5 - \Gamma - \sqrt{16\Gamma + (1 - \Gamma)^2}][6R_2^2 + \Delta(\sqrt{16\Gamma + (1 - \Gamma)^2}) - 4]}{6R_2^2[1 + \Gamma + \sqrt{16\Gamma + (1 - \Gamma)^2}]}. \quad (83c)$$

V. EXPERIMENTAL VERIFICATION OF THE THEORETICAL ENERGETIC HIERARCHY FOR A (2 \times 2)-ELECTRIC CIRCUIT

Just as the steady state characterized by Prigogine is associated with the production of entropy at a minimum constant rate in a system, it also represents the only thermodynamic state whose useful energy to perform work against the surroundings is zero. When we make a distinction between spontaneous and nonspontaneous processes, we can introduce one more constraint to the system that is related to the extrathermodynamic conditions (operation modes). Then all of existing steady states laying between the maximum power output regime and the minimum dissipation regime (minimum entropy production) can be physically attainable.

The validity of the energy conversion theorems as well as their corollaries enunciated and developed in Sec. III is proved through the electric model with resistors previously proposed.

Taking into account the operating conditions imposed by the well-known operating regimes (mdf, MPO, M η , MEF, M Ω , and MP $_{\eta}$), we measure the electric current (driven flux J_1) in mesh 1 of the scheme (see Fig. 5) to reproduce the hierarchical behavior described in Sec. II [see Eqs. (9)]. That is, we are looking for the energetics of the system for different values of the resistor R_2 and, by transitivity, for different values of q which always guarantee that $X_1^{\text{mdf}}[x^{\text{mdf}}(q), q] < X_1^{\text{M}\eta}[x^{\text{M}\eta}(q), q] < X_1^{\text{MEF}}[x^{\text{MEF}}(q), q] < X_1^{\text{M}\Omega}[x^{\text{M}\Omega}(q), q] < X_1^{\text{MP}_{\eta}}[x^{\text{MP}_{\eta}}(q), q] < X_1^{\text{MPO}}[x^{\text{MPO}}(q), q]$.

The nominal resistance values R_2 were calculated to check the existence of the optimal operation regimes by considering 10 different values of $q \in [0.950, 0.995]$, taken in steps of 0.05 (see Table II). This interval is used in analogy to the results reported by Stucki [16], in which he considered that values of $q \in [0.95, 0.97]$ that offer the optimal economic degrees of coupling. For this reason R_1 and R_3 were fixed at a

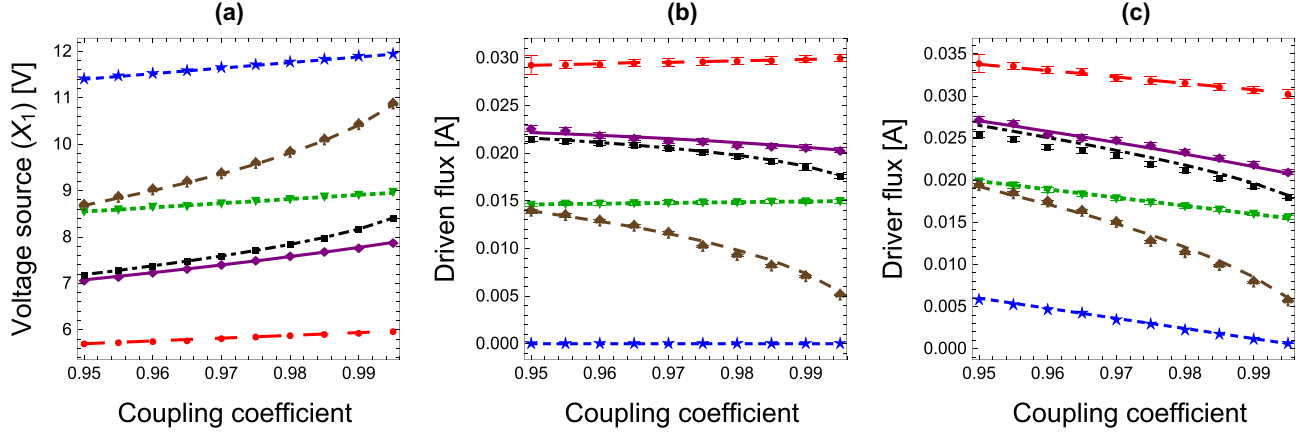


FIG. 6. Graphs of X_1 (source voltage), J_1 (driven flux), and J_2 (driver flux) vs q . The points associated with the experimental measurements for each regime are shown with red circles for MPO, purple diamonds for $MP\eta$, black squares for $M\Omega$, green inverted triangles for MEF, brown spades for $M\eta$, and blue stars for mdf, while theoretical models are depicted by the following curves: dashed (large) red curve for MPO, solid purple curve for $MP\eta$, dot-dashed black curve for $M\Omega$, dotted green curve for MEF, dashed (medium) brown curve for $M\eta$, and dashed (small) blue curve for mdf. In (a) a hierarchy between the different values of X_1 is displayed: (from bottom to top) $X_1^{\text{MPO}} < X_1^{\text{MP}\eta} < X_1^{\text{M}\Omega} < X_1^{\text{MEF}} < X_1^{\text{M}\eta} < X_1^{\text{mdf}}$. In (b) and (c) there are also trends between the operation regimes. They are expressed as the energy consumption in each mesh.

constant value of 100 ohms. By using Eq. (64), we estimated the R_2 values for each q .

The next thing was to consider the triad of values for resistors R_1 , R_2 , and R_3 (see Table II) and a fixed value of $X_2 = 12$ V for the dc voltage source related to the driver flux with the purpose of having completely characterized the steady states. From Eqs. (67), (70), (73), (76), (79), and (82), the values of X_1 were found as a function of any operation mode. Thus, with the values of the resistors R_i and the adjusted values for the dc voltage sources X_k , the assembled electric circuit was put inside a container with dielectric oil to emulate its conditions as an isothermal energy converter and then measure the values of the driven and driver fluxes (electric currents) by considering a long-enough relaxation time (each 5 min approximately) to guarantee their stability (steady states).

In Fig. 6, we display the theoretical and experimental trends that the voltage source X_1 , as well as the electron fluxes J_1 and J_2 , present according to the operating regimes. In the case of X_1 values, they have as upper bound $X_2 =$

12 V (the value of the fixed force). It is important to note that the X_1 values in MPO-regime are almost halved with respect to X_2 . The purpose of the above-mentioned graphs (Fig. 6) is to compare the behavior of (J_1, J_2, X_1) that the linear energy converter model predicts with direct measurements of electric current and voltages through a digital multimeter.

The percentage errors in the measurements for every process variable can be estimated. In the case of power output, the maximum percentage error is calculated for the $M\eta$ regime, its average is $\langle \Delta P_{\%}^{\text{M}\eta} \rangle \approx 6.18\%$. The efficiency presents a maximum mean percentage error when the system works in the $M\Omega$ regime, which is $\langle \Delta \eta_{\%}^{\text{M}\Omega} \rangle \approx 2.75\%$. Finally, the dissipation function has the same maximum error in the $M\Omega$ regime, whose value is $\langle \Delta \Phi_{\%}^{\text{M}\Omega} \rangle \approx 7.98\%$. In general, the foregoing shows that the fluctuations produced by the disturbance of the system (interaction with the measuring instruments) are small. This fact guarantees that the electric circuit reaches a steady state.

Finally, in Fig. 7 the behavior predicted by the theorems proved in Sec. III is depicted for the three process variables. Thus, all the physically attainable operation modes for an isothermal linear energy converter are bounded between the maximum power output and minimum dissipation function regimes, while the optimum operation ones lies between the maximum power output and the maximum efficiency regimes.

VI. CONCLUSIONS

Among the whole set of phenomena that can be described by the so-called steady states, few of them have simple uncoupled processes, i.e., a large number of phenomena have the characteristic of being spontaneous and noninteracting (symmetry principle of Pierre Curie [9]). In fact, living and human-made systems characterized by a single process could be said to undoubtedly satisfy Prigogine's theorem, since this extremal principle considers unconstrained forces and

TABLE II. Resistor R_i (in ohms) and phenomenological coefficients L_{jk} (in siemens) values that correspond to each of the given q values.

q	R_1	R_2	R_3	L_{11}	L_{12}	L_{22}
0.950	100	1900.00	100	0.005128	0.00487	0.005128
0.955	100	2122.22	100	0.005115	0.00488	0.005115
0.960	100	2400.00	100	0.005102	0.00489	0.005102
0.965	100	2757.14	100	0.005008	0.00491	0.005008
0.970	100	3233.33	100	0.005007	0.00492	0.005007
0.975	100	3900.00	100	0.005006	0.00493	0.005006
0.980	100	4900.00	100	0.005005	0.00494	0.005005
0.985	100	6566.67	100	0.005003	0.00496	0.005003
0.990	100	9900.00	100	0.005002	0.00497	0.005002
0.995	100	19900.00	100	0.005001	0.00498	0.005001

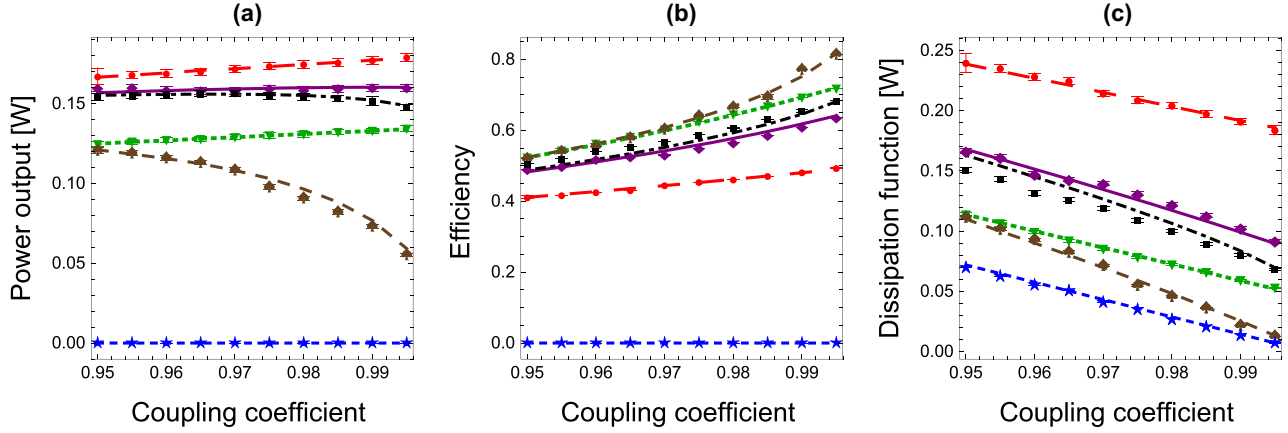


FIG. 7. Graphs of the three process variables vs q . The points associated with the experimental measurements for each regime are shown with red circles for MPO, purple diamonds for $MP\eta$, black squares for $M\Omega$, green inverted triangles for MEF, brown spades for $M\eta$, and blue stars for mdf for (a) power output, (b) efficiency, and (c) dissipation function, while the trend given by the theoretical models are depicted by the following curves: dashed (large) red curve for MPO, solid purple curve for $MP\eta$, dot-dashed black curve for $M\Omega$, dotted green curve for MEF, dashed (medium) brown curve for $M\eta$, and dashed (small) blue curve for mdf.

therefore systems reach a diffusive regime when energy transfer processes are carried out.

There is a divided opinion on the validity of the minimum entropy production theorem and the principle of maximum entropy production, which largely explains all the processes that occur near the equilibrium state. In our opinion, if it is desirable to obtain a useful energy available through certain coupled processes (energy conversion), and that can be mod-

eled to a large extent by means of so-called energy converters within the context of LIT, then one cannot expect a minimum entropy production. Furthermore, we have established optimization criteria that are associated with characteristic steady states that are delimited between the MPO and $M\eta$ operation regimes. That is, other energy conversion theorems can be stated as long as the trade-off between the process variables of the energy converter is well specified.

In the simple experiment that was designed, we show, on the one hand, that the way in which voltage sources (thermodynamic forces) are tuned lead us to establish a unique performance and, on the other hand, that the steady states associated with an energetic objective function are physically accessible. Furthermore, the state described by the minimum dissipation function leads to zero energy conversion.

ACKNOWLEDGMENTS

This work was partially supported by Instituto Politécnico Nacional-México: SIP Projects No. 20221365 and No. 20221415, COFAA Grants No. 5406 and No. 5419, EDI Grants No. 1750 and No. 2248; and SNI-CONAHCYT-México Grants No. 10743 and No. 16051. As well as G. Valencia-Ortega acknowledges the support provided by CONAHCYT-México through the assignment postdoctoral fellowship “Estancias Posdoctorales por México 2022.”

APPENDIX: SOME ALGEBRAIC PROPERTIES OF THE OPTIMAL PERFORMANCE REGIMES

From the definition of entropy production as a function of the force associated to spontaneous flux and the force associated with nonspontaneous flux, the surface Φ characterized by an ordered pair (X_1, X_2) leads us to define a vector space given by the basis vectors $\mathcal{X} = \{(X_1, 0), (0, X_2)\}$. As it is possible to express X_1 as a function of X_2 , then

$$H_{(X_1, X_2)} := \{(X_1, X_2) | X_1 = AX_2, \text{ with } A \text{ a constant and } X_2 \text{ an arbitrary force } \in \mathbb{R}\} \quad (\text{A1})$$

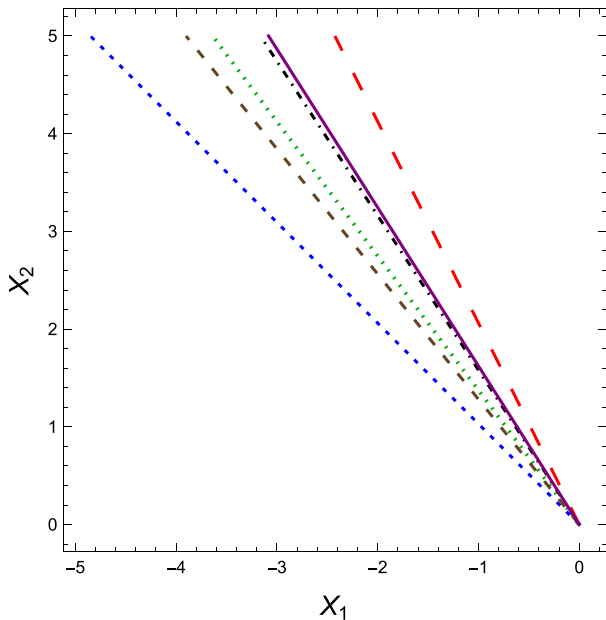


FIG. 8. Graphic sketch of the proper subspace $H_{(X_1, X_2)}$ for different values of $A' = A\sqrt{L_{11}}/\sqrt{L_{22}}$, where X_1 and X_2 are the so-called generalized thermodynamic forces. An order from left to right is noted for the six operation regimes as follows: dashed (small) blue curve for mfd, dashed (medium) brown curve for $M\eta$, dotted green curve for MEF, dot-dashed black curve for $M\Omega$, solid purple curve for $MP\eta$, and dashed (large) red curve for MPO. All lines were depicted under the normalization condition A' and with $q = 0.97$.

defines the proper subspace of such vector space [62]. An energy converter delimits the vector space of these linear irreversible processes in the region with $X_1 < 0$ and $X_2 > 0$. From Eqs. (6) and (8), we note that these optimal operation modes lie in the subspace $H_{(X_1, X_2)}$. That is, according to the physical information of A , a linear energy converter can access different physical realizations as long as the thermodynamic forces are tuned under the respective constraints.

Since the restriction $X_1^Y = A^Y X_2$, with Y the optimal operation mode, is associated with a particular extrathermodynamic condition. In Fig. 8 we can observe the geometric representation of proper subspaces of \mathcal{X} , restricted to the physical region of linear energy converters given by the Eqs. (6) and (8).

The order displayed in Fig. 8 for each operating regime, can be viewed as the availability of a linear energy converter to locate physical realizations when thermodynamic forces are associated in such a way as to achieve a particular goal in energy conversion. That is, if we measure the distance between an arbitrary point (X_1, X_2) and the equilibrium state $(0,0)$ for each proper subspace,

$$d(\vec{0}, \vec{X}) = \|\vec{X} - \vec{0}\| = X_2 \sqrt{1 + (A^Y)^2}, \quad (A2)$$

then we observe that $A^{\text{MPO}}[x^{\text{MPO}}(q), q] < A^{\text{MP}\eta}[x^{\text{MP}\eta}(q), q] < A^{\text{M}\Omega}[x^{\text{M}\Omega}(q), q] < A^{\text{MEF}}[x^{\text{MEF}}(q), q] < A^{\text{M}\eta}[x^{\text{M}\eta}(q), q] < A^{\text{mdf}}[x^{\text{mdf}}(q), q]$ and therefore the distances reveal the same order as inequalities [see Eq. (9)].

-
- [1] I. Prigogine, *Etude thermodynamique des phénomènes irréversibles*, 1st ed. (Desoer, Liège, 1947).
- [2] R. J. Tykodi, *Thermodynamics of Steady States*, 1st ed. (The Macmillan Company, New York, 1967).
- [3] E. T. Jaynes, *Ann. Rev. Phys. Chem.* **31**, 579 (1980).
- [4] M. M. Mamedov, *Tech. Phys. Lett.* **29**, 340 (2003).
- [5] L. M. Martyushev, A. S. Nazarova, and V. D. Seleznev, *J. Phys. A: Math. Theor.* **40**, 371 (2007).
- [6] V. Bertola and E. Cafaro, *Int. J. Heat Mass Transf.* **51**, 1907 (2008).
- [7] L. M. Martyushev, *Entropy* **15**, 1152 (2013).
- [8] L. Onsager, *Phys. Rev.* **37**, 405 (1931).
- [9] D. Kondepudi and I. Prigogine, *Modern Thermodynamics: From Heat Engines to Dissipative Structures*, 2nd ed. (John Wiley & Sons, Chichester, 2015), p. 391.
- [10] I. Ráfols and J. Ortín, *Am. J. Phys.* **60**, 846 (1992).
- [11] I. Danielewicz-Ferchmin and A. Ryszard Ferchmin, *Am. J. Phys.* **68**, 962 (2000).
- [12] D. Lurié and J. Wagensberg, *Am. J. Phys.* **48**, 868 (1980).
- [13] M. J. Klein and P. H. E. Meijer, *Phys. Rev.* **96**, 250 (1954).
- [14] H. B. Callen, *Thermodynamics and an Introduction to Thermostatistics*, 2nd ed. (John Wiley & Sons, New York, 1985).
- [15] F. Mandl, *Statistical Physics*, 2nd ed. (John Wiley & Sons, Manchester, 1991).
- [16] J. W. Stucki, *Eur. J. Biochem.* **109**, 269 (1980).
- [17] S. R. Caplan, and A. Essig, *Bioenergetics and Linear Nonequilibrium Thermodynamics*, 1st ed. (Harvard University Press, Cambridge, UK, 1983).
- [18] L. A. Arias-Hernandez, F. Angulo-Brown, and R. T. Paez-Hernandez, *Phys. Rev. E* **77**, 011123 (2008).
- [19] F. Angulo-Brown, M. Santillán, and E. Calleja-Quevedo, *Nuovo Cimento Soc. Ital. Fis. D* **17**, 87 (1995).
- [20] M. Santillán, L. A. Arias-Hernandez, and F. Angulo-Brown, *Nuovo Cimento Soc. Ital. Fis. D* **19**, 99 (1997).
- [21] L. Onsager, *Phys. Rev.* **38**, 2265 (1931).
- [22] H. B. Callen, *Phys. Rev.* **73**, 1349 (1948).
- [23] H. T. Odum and R. C. Pinkerton, *Am. Sci.* **43**, 331 (1955).
- [24] A. Fronczak, P. Fronczak, and J. A. Holyst, *Phys. Rev. E* **76**, 061106 (2007).
- [25] M. V. Volkenstein, *General Biophysics*, 1st ed. (Academic Press, London, 1983).
- [26] K. Sekimoto, *Stochastic Energetics*, Lecture Notes in Physics, Vol. 799 (Springer, Berlin, 2010).
- [27] S. Sasa and H. Tasaki, *J. Stat. Phys.* **125**, 125 (2006).
- [28] G. Valencia-Ortega and L. A. Arias-Hernandez, *J. Non-Equilib. Thermodyn.* **42**, 187 (2017).
- [29] S. Gonzalez-Hernandez and L. A. Arias-Hernandez, *J. Non-Equilib. Thermodyn.* **44**, 315 (2019).
- [30] G. Valencia-Ortega and L. A. Arias-Hernandez, *Physica E* **124**, 114231 (2020).
- [31] S. R. de Groot, and P. Mazur, *Non-Equilibrium Thermodynamics*, 1st ed. (North-Holland, Amsterdam, 1962).
- [32] I. Prigogine, *Thermodynamics of Irreversible Processes*, 1st ed. (Wiley-Interscience, New York, 1967).
- [33] L. García-Colín and P. Goldstein-Menache, *Procesos Irreversibles: Teoría y Aplicaciones*, Vol. 1, 1st ed. (El Colegio Nacional, Mexico City, 2013).
- [34] L. A. Arias-Hernandez and F. Angulo-Brown, *J. Appl. Phys.* **81**, 2973 (1997).
- [35] M. Tribus, *Thermostatistics and Thermodynamics*, 1st ed. (Van Nostrand, Princeton, NJ, 1961).
- [36] A. C. Hernandez, A. Medina, J. M. M. Roco, J. A. White, and S. Velasco, *Phys. Rev. E* **63**, 037102 (2001).
- [37] F. Angulo-Brown, *J. Appl. Phys.* **69**, 7465 (1991).
- [38] T. Yilmaz, *J. Energy Inst.* **79**, 38 (2006).
- [39] L. Chen and F. Sun, *Advances in Finite Time Thermodynamics: Analysis and Optimization*, 1st ed. (Nova Science, New York, 2004).
- [40] Y. Apertet, H. Ouerdane, C. Goupil, and Ph. Lecoeur, *Phys. Rev. E* **88**, 022137 (2013).
- [41] C. R. Martinez-Garcia, Algunos teoremas análogos al de Prigogine para un sistema de n-flujos y n-fuerzas, Master's thesis, Instituto Politécnico Nacional, 2008.
- [42] J. M. Gordon and M. Huleihil, *J. Appl. Phys.* **72**, 829 (1992).
- [43] S. Carnot, *Reflections on the Motive Power of Heat and on Machines Fitted to Develop That Power*, 2nd rev. ed. (edited by R. H. Thurston, from the original french, John Wiley & Sons, New York, Chapman & Hall, London, 1897), p. 126. Based on what Carnot exposed on this page, he introduces what we currently know as the optimization process, which does not depend on the converter model (FTT, TFS, TFD, LIT, etc.). In general, the performance of actual energy converters is between the point of maximum output power and the point of maximum efficiency, this part of the loop is called the *economic zone* of

- interest* (EZI) (see region from red circle to brown spade of Fig. 2) and this implies to consider aspects such as the price per kilowatt-hour, the initial investment, the size of the converter, the frequency of maintenance, etc. These items are what we call extrathermodynamic conditions.
- [44] S. Levario-Medina, G. Valencia-Ortega, and M. A. Barranco-Jiménez, *J. Non-Equilib. Thermodyn.* **45**, 269 (2020).
- [45] D. G. Miller, *Chem. Rev.* **60**, 15 (1960).
- [46] H. J. M. Hanley, *J. Macromol. Sci. B* **3**, 365 (1969).
- [47] P. Županović, D. Juretic, and S. Botric, *Phys. Rev. E* **70**, 056108 (2004).
- [48] O. Kedem and S. R. Caplan, *Trans. Faraday Soc.* **61**, 1897 (1965).
- [49] F. Angulo-Brown, L. A. Arias-Hernandez, and M. Santillán, *Rev. Mex. Fis.* **48 S1**, 182 (2002).
- [50] V. M. Castillo, W. G. Hoover, and C. G. Hoover, *Phys. Rev. E* **55**, 5546 (1997).
- [51] W. G. Hoover, *Am. J. Phys.* **70**, 452 (2002).
- [52] M. Santillán, G. Maya, and F. Angulo-Brown, *J. Phys. D: Appl. Phys.* **34**, 2068 (2001).
- [53] L. Guzmán-Vargas, I. Reyes-Ramírez, and N. Sánchez, *J. Phys. D: Appl. Phys.* **38**, 1282 (2005).
- [54] Y. Huang, and D. Sun, *J. Non-Equilib. Thermodyn.* **33**, 61 (2008).
- [55] P. A. N. Wouagfack, G. F. Keune, and R. Tchinda, *Int. J. Refrig.* **75**, 38 (2017).
- [56] J. Gonzalez-Ayala, J. Guo, A. Medina, J. M. M. Roco, and A. C. Hernandez, *Phys. Rev. Lett.* **124**, 050603 (2020).
- [57] J. S. Lee, J. M. Park, H. M. Chun, J. Um, and H. Park, *Phys. Rev. E* **101**, 052132 (2020).
- [58] G. Valencia-Ortega, S. Levario-Medina, and M. A. Barranco-Jiménez, *Physica A* **571**, 125863 (2021).
- [59] P. Glansdorff, and I. Prigogine, *Physica* **20**, 773 (1954).
- [60] P. Glansdorff and I. Prigogine, *Thermodynamic Theory of Structure, Stability and Fluctuations*, 1st ed. (Wiley-Interscience, London, 1971).
- [61] G. Nicolis and I. Prigogine, *Self-organization in Nonequilibrium Systems*, 1st ed. (John Wiley & Sons, New York, 1977).
- [62] S. I. Grossman, *Elementary Linear Algebra*, 5th ed. (Thomson Learning, Stamford, CT, 1994).